exosat esa

EXOSAT EXPRESS

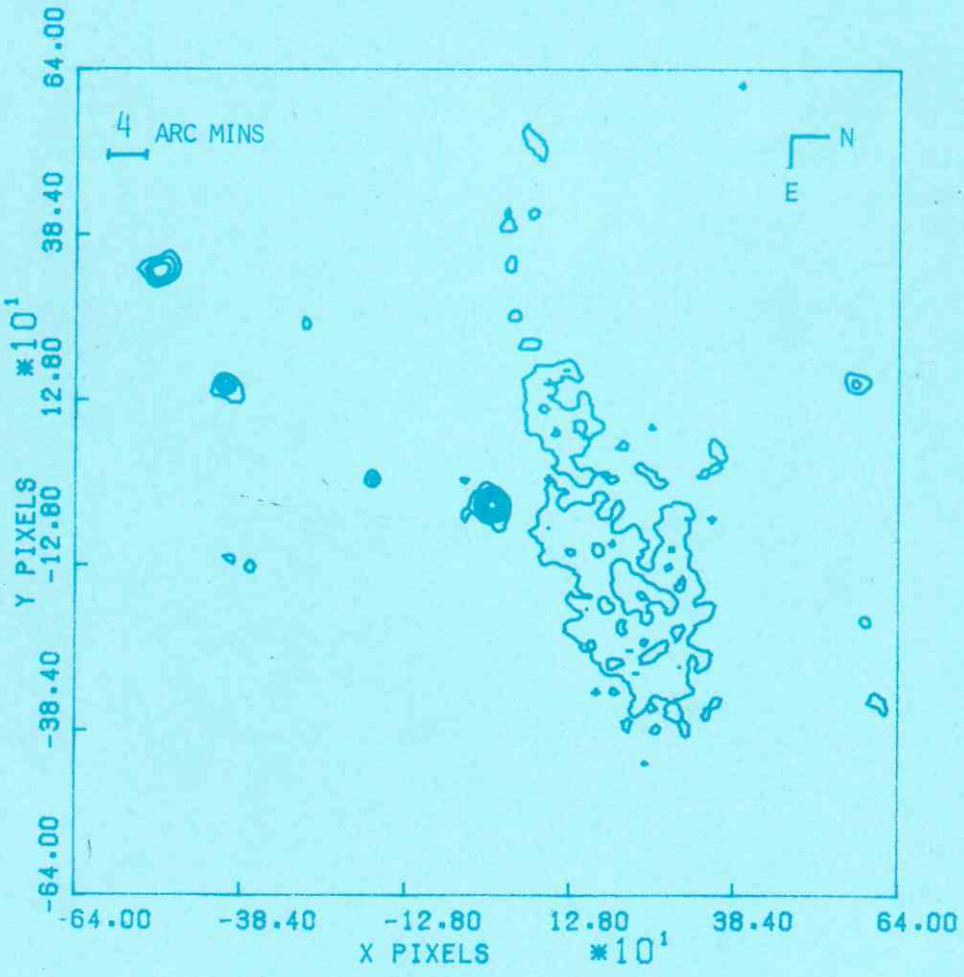

EXOSAT
EUROPEAN X-RAY ASTRONOMY SATELLITE

No. 8

Dezember 1984

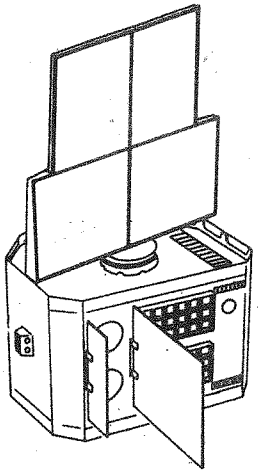

esa

EXOSAT EXPRESS

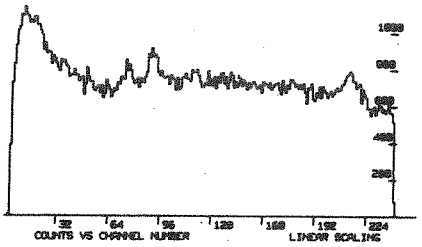

TABLE OF CONTENTS

NO. 8 DECEMBER 1984

Front Cover

A CMA image, obtained using the 3000 Å Lexan filter, of the region close to the VELA pulsar (PSR0833-45), which is visible slightly south of the bright ridge of emission.

Courtesy : A. Smith

FOREWORD

The EXOSAT Interactive Analysis System has been operational on a trial basis at the Observatory since 1st December 1984. Initial experience of the observatory group and a number of first time users has proved invaluable in highlighting areas for improvement. Our intention is to continue the trial period informally for a short time during which additional facilities will be added with considerable effort devoted to documentation. Users are reminded of the booking procedure (EXPRESS no. 7 p. 43/44) and attention is drawn to a short description of the current facilities (p. 33).

On day 366 a malfunction in the operation of the X-gyro occurred (details on p. 2). Since then the redundant Skew (S) gyro has been used for spacecraft pointing and control. A failure investigation and definition of further backup procedures are in progress.

A review of the papers presented at the ESLAB Symposium is given on p. 16 followed by a summary of the topics covered and main discussion areas at the Data Analysis Workshop. Subject to the level of interest from the community, ESA intends to hold a second data analysis workshop at ESOC (ref. p. 24). Comments on the first workshop - level of presentation, choice of material etc. - and desirability of a repeat would be highly appreciated.

Selection of the AO-3 programme of observations will be carried out by the Committee on Observation Proposal Selection (COPS) at their meeting on 4-7 February 1985.

EXOSAT EXPRESS

Editor: David Andrews

Published by: EXOSAT Observatory,
ESOC,
Robert Bosch Strasse 5,
6100 Darmstadt,
West Germany.

Tel: 06151-886-704
Telex: 419453/49441
Telefax: 886/622/611

OBSERVATORY STATUS AS OF 31.12.84

EXOSAT's third programme of observations (AO-3) will start during February/March 1985 and has a planned duration of 12 months. Outstanding AO-2 pointings (~110 of the 470 approved) will be completed in January/February or interleaved with the AO-3 programme.

1. Hardware

At 09.18Z on Day 366(84) the X-gyro motor current increased from its nominal value of ~70 ma to ~200 ma within one telemetry format (8s). The current remained high, fluctuating between ~180 ma and 276 ma (full scale on the analogue read out) and the X-gyro health monitor switched from 'GOOD' to 'FAIL'. Since gyro selection was on the basis of the health monitor, the S (Skew)-gyro was autonomously selected. De-pointing of the spacecraft occurred on all three axes as a result of the S-gyro selection. Periodic switching on of the X-gyro heater by its temperature control circuit was observed for several minutes after the gyro motor current increase, however this behaviour ceased and a short time later the temperature of the gyro box increased. On this basis, the gyro selection logic was changed from 'health monitor' to "SYZ" and the X-gyro switched off. Safety mode was triggered at this point (Y-axis pointing at the sun) with an indication that excessive rate had been detected but this was later diagnosed as spurious incremental signals generated by the X-gyro switch off.

A short test of the X-gyro was carried out while the spacecraft remained in safety mode. The gyro was switched on for approximately 7 minutes, throughout which the motor displayed a similar behaviour as earlier and the health monitor remained at 'FAIL'. During the switch on and off the Y-axis rotation rate changed, consistent with a momentum exchange between the spacecraft and X-gyro on the assumption that the X-gyro was spinning at its nominal rate.

There have been no changes in the status of the payload hardware. Additional calibration tests on the GSPC (ref. p. 25) have led to refinement of the effective areas and a re-definition of the background line feature energies.

2. Performance and Operation

Tables 1 and 2 on p. 5/6 give the current performance parameters of the EXOSAT instruments.

During the period 1.11.84 to 31.12.84 loss of observation time has resulted from ground computer system problems (3 hrs, Day 310), a power failure at ESOC (3 hrs, Day 334), solar activity (3.6 hrs, Day 355) and the X-gyro malfunction on day 366 (~16 hrs).

Regular swapping of the ME detector array halves was re-introduced (ref. EXPRESS no. 6 p. 4) to provide optimal background subtraction for weak source observations. This procedure is now the default for all observations, and P.I.'s should inform the Duty Scientist responsible for the orbit preparation if array swapping is not required.

A number of problems have arisen during source observations with respect to the requested payload configuration or OBC modes, e.g. a detection of a weak extragalactic source with the Boron filter without first using the Lexan filters. The following general configuration conditions are considered as standard:

i) Medium energy experiment array half is always offset with an array swap as above (typically once/unit).

ii) Weak sources must be observed initially with a Lexan filter and detected.

iii) Photometry using the low energy telescope will be performed only with a Lexan filter.

Note that responsibility for the final decision on configuration rests with the Duty Scientist/Observatory Controller who will be familiar with the science of the proposal and all payload/OBC operational details.

3. Observation Output

P.I.'s are reminded that the Observatory will despatch 1 copy only of the FOT per observation. There are no exceptions to this rule and P.I.'s must themselves ensure the distribution of data as appropriate to their Co.I.'s.

Chapter 8.2 of the revised (Rev. 2) FOT Handbook, dealing with ME data analysis, will be despatched shortly together with a number of single page updates to Rev. 2.

Future Plans

A 'natural' occultation of 4U1530-44 is scheduled for 16.01.85. This will provide a thorough test of the ground system software and operations procedures necessary to carry out occultations. Following this, a decision will be taken on the execution of a small number of approved AO occultation observations.

Specification of the concept and design of software for the generation of the EXOSAT observation log is in progress. The function of this log is to provide a ready means to inform the community of the EXOSAT observation programme and to enable the Observatory Team to request information about this programme.

Software implementation and generation of the log is planned for early summer 1985, such that public access to EXOSAT data can be supported in an efficient manner.

Data from PV/Cal and certain AO-1 observations will become public in April 1985. The observation log will identify which data is currently available and listings will be published in the EXPRESS.

TABLE 1

PERFORMANCE CHARACTERISTICS (LE)

LE1	Characteristics			
Energy Range	0.04-2 keV (6-300 A) CMA*			
	0.3 - 2 keV PSD			
Energy resolution	Five filters are available for broad-band spectroscopy (CMA)			
	$(\Delta E/E) = 41/E(keV)^{0.5}$ %FWHM (PSD)			
Field of view	2.2° diameter (CMA) 1.5° diameter (PSD)			
Effective area (cm^2)	Thin Lexan Filter	Al/P Filter	Boron Filter	Open position (PSD)
.05 keV	0.4	2.6	-	-
.1 keV	11.1	0.4	-	-
.5 keV	4.5	3.3	0.4	1.9
1.0 keV	3.2	2.5	2.0	13.5
1.5 keV	2.2	1.6	1.8	9.7
2.0 keV	0.6	0.5	0.6	1.9
Spatial resolution (Line spread function HEW)				
On axis :	18 arc sec (CMA)		3 arc min (PSD)	
20 arc minutes off-axis:	40 arc sec (CMA)		3.5 arc min (PSD)	
Average steady residual background**	1.8 cnts/sec/cm^2 (CMA)			
	0.7 cnts/sec/cm^2/kev (PSD)			

* Subject to UV contamination between 900 - 2600 A
** Background rate subject to flaring

TABLE 2

PERFORMANCE CHARACTERISTICS (ME & GSPC)

Medium Energy Experiment	Characteristics
Total effective area	1500 cm^2 (all quadrants co-aligned)
Effective energy range	1-20 keV (Argon proportional counters) 5-50 keV (Xenon proportional counters)
Energy resolution ($\Delta E/E$)	$51/E\ (kev)^{1/2}$ % FWHM (Argon counters) 18% for 10 keV$\leq E \leq$ 30 keV (Xenon counters)
Field of view	45 arc minutes FWHM, triangular response with a 3' flat top
Total residual background	4 cnts/sec/keV (2-10 keV Argon counters co-aligned)
Gas Scintillation Counter (GSPC)	
*Total effective area	$\sim$100 cm^2 (ref. p. 26)
Effective energy range	2-18 keV or 2-40 keV, depending on gain setting
Energy resolution ($\Delta E/E$)	$27/E\ (kev)^{1/2}$ % FWHM
Field of view	45 arc minutes FWHM triangular response with a 3' flat top
Total residual background rate	1.3 cnts/sec/keV (2-10 keV)

* depends on E and burst length window setting

AO-2 OBSERVATIONS 01.11.84 - 31.12.84

Day (84)	Time	Target	RA	Dec	SAA	Duration h m	Principal Investigator	
306	06.33	A576	07 17 38	+55 53 31	111	6 46	Mushotzky	
306	15.35	MGC 8-11-11	05 51 18	+46 28 22	126	3 15	Maraschi	
306	21.00	GW00747+553	07 47 39	+55 21 54	107	3 0	Bradt	
307	03.23	MR2251-178	22 51 21	-17 54 01	117	6 6	Pounds	
307	11.50	SMC X-1	01 15 14	-73 43 54	90	3 30	Watson	
307	18.01	Cyg X-1	19 56 21	+35 01 02	91	5 50	Page	
308	01.48	MKN 180	11 31 09	+70 25 21	90	3 41	Warwick	
308	09.40	VW Hydri	04 09 30	-71 25 23	92	6 39	Pounds	AO-1
308	17.38	LMC X-3	05 39 10	-64 06 38	93	2 57	Van der Klis	
308	23.40	4U0614+09	06 14 34	+09 11 07	126	5 28	Mason	
310	05.34	NGC 2110	05 49 59	-07 16 55	127	5 29	Pounds	
310	13.15	PK219+31.1	08 51 43	+09 07 00	90	3 2	De Korte	
310	18.45	MR 374	06 55 46	+54 18 43	118	7 28	Bergeron	
311	09.09	HD203387	21 19 21	-17 05 49	93	2 56	Praderie	
311	13.43	PKS2155-304	21 55 52	-30 30 54	96	4 4	Tanzi	
311	19.46	GL 876	22 50 30	-14 34 17	114	4 1	Schmitt	
312	02.10	NGC7213	22 06 07	-47 28 05	90	6 27	Pounds	
312	09.48	PKS2155-304	21 55 52	-30 30 54	95	3 59	Tanzi	
312	16.38	4U0614+09	06 14 34	+09 11 03	129	7 42	Mason	
313	16.45	S50014+81	00 13 05	+81 18 42	113	21 31	Zimmermann	
314	17.02	4U0027+59	00 26 42	+59 29 57	129	3 16	Van Paradijs	
314	23.10	IH1013+498	10 17 40	+49 34 51	90	3 7	Schwartz	
315	04.29	0855+143	08 56 04	+14 22 21	95	13 9	Bregman	
315	19.50	NGC7314	22 32 57	-26 20 04	101	5 43	Pounds	AO-1
316	02.30	MR2251-178	22 51 22	-17 52 58	108	7 8	Pounds	
316	11.24	PKS2155-304	21 55 53	-30 29 51	91	3 19	Tanzi	
316	16.50	GD 394	21 10 54	+49 51 55	104	3 09	Heise	
317	08.54	G78.2+2.1	20 21 24	+40 13 50	92	9 59	Peacock	
317	20.50	MKN180	11 30 58	+70 25 42	96	2 40	Warwick	
318	00.35	3C263	11 37 32	+66 04 36	92	3 35	Smith	
318	06.25	CRAB	05 31 32	+21 58 34	147	2 40	GSPC Cal.	
318	11.30	H0139-68	01 39 17	-68 10 25	92	6 7	TOO	
318	20.01	HD100696	11 29 59	+69 36 29	96	5 12	Bedford	AO-1
319	03.15	YY Gem	07 31 34	+32 00 18	121	20 56	Gibson	
320	04.30	N103B	05 09 44	-68 48 39	90	10 05	Schnopper	
321	06.26	MCG2-58-22	23 02 05	-08 59 58	109	6 6	Pounds	AO-1
321	14.56	II ZW136	21 29 58	+09 52 23	94	6 5	Bergeron	
321	22.56	1003+35	10 03 15	+35 10 25	93	3 6	Miller	AO-1
322	03.40	Sigma Gem	07 40 18	+29 02 30	122	9 11	Schnopper	AO-1
322	15.43	Nova Vul 84	19 24 03	+27 16 42	73	5 34	Ögelman	
322	23.40	MCG2-58-22	23 02 04	-08 59 40	107	3 11	Scarsi	
323	03.55	Gliese 867	22 35 59	-20 55 28	97	4 6	Jensen	
323	10.25	H0534-58	05 34 22	-58 03 43	98	8 7	Tuohy	
323	20.45	Sigma Gem	07 40 18	+29 02 31	124	3 56	Schnopper	AO-1

Day (84)	Time	Target	RA	Dec	SAA	Duration h m	Principal Investigator	
325	06.15	MKN180	11 31 03	+70 25 54	99	3 13	Warwick	
325	13.00	MR2251-178	22 51 20	-17 53 28	99	5 30	Pounds	
325	19.30	MCG2-58-22	23 02 00	-08 59 32	105	3 16	Scarsi	
326	02.26	Sigma Gem	07 40 21	+29 02 01	126	8 57	Schnopper	A0-1
326	12.50	GL 388	10 17 05	+20 08 12	90	3 22	De Korte	
326	18.04	1053+70	10 54 00	+70 28 44	103	6 0	Witzel	
327	03.08	MCG2-58-22	23 02 00	-08 59 32	103	3 9	Scarsi	
327	08.39	A 140	01 02 04	-24 16 50	119	4 28	McKechnie	
327	16.08	LMC X-1	05 40 35	-69 47 15	88	2 59	Ilovaisky	
327	20.19	RR PIC	06 35 34	-62 36 25	91	4 17	Van der Woerd	
328	14.30	LMC X-1	05 40 33	-69 47 06	78	7 0	Ilovaisky	
328	23.55	IH0712+558	07 12 32	+55 51 40	129	2 20	Wood	
329	05.10	CPD-48 1577	08 14 04	-49 03 30	90	3 7	Williams	
329	10.44	MCG2-58-22	23 03 01	-08 59 24	101	3 33	Scarsi	
329	16.23	WD0500-33	00 54 16	-33 17 13	110	3 19	Heise	
329	23.00	CPD-48 1577	08 14 04	-49 03 40	90	9 2	Williams	
330	10.10	LB 1663	03 23 57	-54 45 43	104	3 38	Kahn	
330	15.00	Fairall 9	01 21 52	-59 06 37	93	7 3	Pounds	A0-1
331	00.35	A119	00 53 44	-01 34 29	127	8 13	Morini	
331	11.05	Feige 108	23 13 31	-02 09 23	104	3 10	Heise	
331	15.09	MCG 2-58-22	23 02 01	-08 59 23	99	7 23	Scarsi	
332	11.40	MR2251-178	22 51 23	-17 53 28	92	6 26	Pounds	
332	19.33	NGC7469	23 00 40	+08 33 46	104	7 2	Pounds	A0-1
333	04.44	MKN 180	11 33 41	+70 28 35	103	4 47	Warwick	
333	10.45	I 691	11 24 11	+59 27 04	100	6 51	Peacock	
333	18.44	NGC 3642	11 19 42	+59 22 18	100	4 2	Peacock	
334	01.50	3A0726-260	07 27 01	-25 59 38	114	9 39	Corbet	
334	13.50	BV Pup	07 47 09	-23 25 40	112	3 39	Szkody	
334	20.02	PG0956+35	09 56 10	+35 55 40	107	2 58	Heise	
335	00.02	GL 411	11 00 48	+36 16 52	95	2 49	Schmitt	
335	04.35	A1318	11 33 58	+55 16 13	98	6 6	McKechnie	
335	11.48	PG1210+533	12 11 11	+53 21 34	92	3 12	Heise	
336	07.14	G109.1-1.0	22 58 46	+58 34 41	112	22 59	Morini	
337	08.51	TY Pyx	08 58 01	-27 36 25	99	4 52	White	
337	17.05	MKN 421	11 01 55	+38 29 46	98	3 13	Bowyer	
337	23.00	NGC 2992	09 43 29	-14 04 47	96	3 48	Pounds	
338	04.00	RW Sex	10 17 38	-08 25 52	91	3 43	Van der Woerd	
338	10.13	3A2356-341	23 54 20	-35 05 09	91	6 20	Schwartz	
338	19.13	MKN 421	11 01 55	+38 39 48	99	6 55	Bowyer	
339	05.15	EZ Cam	06 52 21	-23 52 26	124	5 39	Willis	
340	05.52	G127.1+0.5	01 24 42	+62 49 12	127	11 18	Peacock	
340	19.13	MKN 421	11 01 50	+38 29 42	101	3 17	Bowyer	
341	02.04	UV Ceti	01 36 24	-18 14 50	117	8 46	Butler	
341	13.52	MKN 335	00 03 41	+19 53 34	113	8 58	Pounds	
341	23.55	EQ Peg	23 29 16	+19 37 44	105	10 39	Butler	
342	14.05	Gamma Cas	00 53 27	+60 25 32	123	5 30	Frontera	

Day (84)	Time	Target	RA	Dec	SAA	Duration h m	Principal Investigator	
342	21.25	3A2206+543	22 06 02	+54 14 21	101	4 37	Watson	
344	04.45	OJ 287	08 52 05	+20 19 05	127	8 20	Pollock	
344	15.10	PK261+32.1	10 22 30	-18 22 42	92	2 50	de Korte	
344	19.05	NGC 2992	09 43 26	-14 05 08	102	5 15	Pounds	
345	02.59	0855+143	08 56 04	+14 22 20	125	12 7	Bregman	
345	16.55	OJ 287	08 52 05	+20 19 05	128	9 25	Pollock	
346	05.10	1156+295	11 57 07	+29 34 04	92	3 19	McHardy	
346	11.17	HD36705	05 28 35	-65 19 19	91	1 47	Rucinski	
347	13.49	LMX X-3	39 01 29	-64 08 00	92	5 42	Van der Klis	
347	21.55	PG 1034+001	10 34 39	+00 08 37	100	3 55	Heise	
348	04.25	3C263	11 37 29	+66 06 15	109	14 35	Smith	
348	20.10	GD 323	13 02 50	+59 44 30	98	6 35	Heise	
349	02.00	1044+71	10 45 09	+72 01 48	115	6 35	Witzel	
349	10.43	1826+79	18 27 21	+79 34 46	103	6 1	Witzel	
349	19.12	PHL909	00 54 28	+14 27 22	115	7 15	Stewart	AO-1
350	05.30	LMC X-3	05 39 00	-64 08 08	92	4 50	van der Klis	
350	11.45	3A 0557-383	05 56 33	-38 21 37	118	7 25	Pounds	
351	11.00	NGC 4151	12 08 13	+39 42 13	98	2 50	Perola	
351	16.15	H0917-074	09 20 48	-07 48 00	116	2 9	Lawrence	
351	19.05	H0917-074	09 13 12	-07 05 59	118	3 3	Lawrence	
351	22.46	H0917-074	09 17 11	-07 26 05	118	8 15	Lawrence	
352	10.30	3A0234-526	02 36 43	-52 27 21	94	6 35	Pye	AO-1
352	18.51	IH0900-48	08 58 17	-47 55 36	96	1 24	PV/Cal	
352	20.52	IH0900-48	09 02 53	-48 26 45	95	2 0	PV/Cal	
352	23.40	IH0900-48	08 54 29	-47 29 50	96	1 0	PV/Cal	
353	01.24	IH0900-48	09 05 19	-48 26 59	95	2 36	PV/Cal	
353	05.15	VELA X-1	09 00 28	-40 21 11	101	10 49	Peacock	AO-1
353	18.50	NGC 2992	09 43 28	-14 04 50	110	3 58	Pounds	
354	01.05	LMC X-3	05 38 59	-64 08 29	92	3 43	Treves	
354	07.40	NGC 4151	12 08 13	+39 42 18	101	4 9	Perola	
355	07.11	1114+18	11 14 49	+18 14 46	105	6 48	Biermann	
355	17.10	0008+70	00 08 24	+70 27 09	113	5 55	Witzel	
356	00.15	0027+70	00 26 48	+70 19 51	114	6 50	Witzel	
356	08.52	2010+72	20 10 18	+72 17 35	98	7 13	Witzel	
356	18.25	2A1219+305	12 19 04	+30 27 47	97	3 25	Warwick	
357	00.48	NOVA MUSCAE	11 50 01	-66 54 39	69	3 27	Krautter	
357	07.15	NGC 4151	12 08 10	+39 42 48	103	5 15	Perola	
357	16.10	NGC526A	01 21 54	-35 20 29	91	5 24	Turner	AO-1
357	23.40	LMC X-1	05 40 20	-69 48 28	86	4 10	Ilovaisky	
358	04.37	LMC X-3	05 38 51	-64 09 01	92	4 29	Treves	
359	03.27	NGC 2992	09 43 27	-35 05 44	115	3 45	Pounds	
359	09.51	NGC 4151	08 12 53	+39 42 06	105	3 16	Perola	
359	14.51	COMA CLU	13 00 58	+28 11 23	90	6 17	Goerenstein	
359	22.12	COMA CLU	12 57 29	+28 11 24	91	3 32	Goerenstein	
360	02.40	COMA CLU	12 54 00	+28 11 24	92	6 30	Goerenstein	
360	10.46	COMA CLU	12 57 29	+28 29 24	91	9 15	Goerenstein	

Day (84)	Time	Target	RA	Dec	SAA	Duration h m	Principal Investigator
360	21.10	M87	12 28 56	+12 41 09	92	12 11	PV/Cal
361	12.20	LMC X-3	05 38 54	-64 08 47	92	3 27	Treves
361	18.30	A 193	01 22 25	+08 24 32	107	7 09	McKechnie
363	00.49	0740+76	07 40 04	+76 48 53	125	6 16	Witzel
363	09.41	NGC 4151	12 08 11	+39 42 25	108	8 6	Perola
363	20.50	NGC 185	00 36 04	+48 01 18	108	8 15	Weisskopf
364	07.23	M31	00 39 54	+40 57 33	106	14 2	van der Klis
365	01.28	NGC 2992	09 43 27	-14 05 09	120	3 17	Pounds
365	07.24	BURST WATCH	05 26 09	-66 09 15	89	14 05	Staubert

TOO : Target of Opportunity

NB : Observation durations are the time from outer loop closure to outer loop opening and should not be considered as necessarily definitive.

: RA, Dec figures quoted in the above list and in all other listings in EXPRESS nos. 1-7 are the star tracker pointing, accurate to 2 or 3 arc seconds. Source positions are typically 2' from this (offset to avoid the detector FOV centre) with superimposed misalignment and randomisation (avoid excess count rates per pixel) effects.

EXOSAT X-RAY SOURCES

'New' X-ray sources are discovered by EXOSAT serendipitously in the FOV of the telescope or in the offset quadrants of the ME or from an analysis of ME/GSPC 'background' data recorded during manoeuvres. We intend to maintain a list of published 'new' sources and readers are encouraged to report 'discoveries'.

It is recommended that the following convention be used when referring to EXOSAT sources in publications; in any case, this format will be adopted for any list maintained by the Observatory Team and is consistent with the recommendations referenced (below) and the Einstein HRI format.

Please note that this convention supercedes and renders obsolete the definition printed in Express issues 4 to 6.

EXOSAT Source Nomenclature

Source Position:	RA	02H	30m	20.5s	(1950)
	DEC	-02D	20m	33.2s	

Name : EXO 023020-0220.5

Ref.(1) Dictionary of the Nomenclature of Celestial Objects
M.C. Lortet and F. Spite, Observatoire de Paris, Meudon

(2) IAU Sub-Group on Nomenclature Problems

IAU (EXOSAT) TELEGRAMS

Circular No.	Title	Comment	Authors
3841	Hercules X-1	Anomalous X-ray behaviour	EXOSAT Team
3842	Supernova in NGC 5236	Multi-waveband observations	W. Wamsteker
3850	GK Persei	351s periodicity during an outburst	M. Watson, A. Smith EXOSAT Team
3854	MXB 1730-335	Active, type 1 bursts	G. Pollard, N. White P. Barr, L. Stella
3858	4U 1543-45	Accurate position, ultra-soft spectrum	R. Blissett, EXOSAT Team
3872	GX 1+4	Unexpected low X-ray state: $\leqslant$ 4 UFU	R. Hall, J. Davelaar EXOSAT Team
3882	4U1755-33	Periodic dips in intensity	N. White, A. Parmar K. Mason
3887	4U2129+47 = V1727 Cygni	Unexpected low X-ray and optical state	W. Pietsch, H. Steinle M. Gottwald
3893	V0332+53	Accurate position, and flux	J. Davelaar, R. Blissett, L. Stella M. McKay, N. White, J. Bleeker
3902	V0332+53	Discovery of 4.4s period	L. Stella, N. White
3906	V0332+53	Unexpected brightening	A.N. Parmar R.J. Blissett T. Courvoisier L. Chiappetti
3912	V0332+53	Orbital parameters determination	N. White, J.Davelaar, A.N. Parmar, L. Stella M. van der Klis

Circular No.	Title	Comment	Authors
3923	Her X-1	Her X-1 'on' again at 80 Uhuru flux units, 1.24s pulsations (March 1.5 - 1.8)	J. Trümper, P. Kahabka H. Ögelmann, W. Pietsch, W. Voges, M. Gottwald, A. Parmar
3932	2S1254-690	Discovery of type 1 Burst and an absorption 'event'.	T. J.-L. Courvoisier, A. Peacock, M. Pakull
3935	AN URSAE MAJORIS	Serendipitous observation: soft X-ray flux suggests a return to the 'bright' state.	J.P. Osborne
3939	VW HYDRI	Discovery of X-ray pulsations during superoutburst	J. Heise, F. Paerels, H. van der Woerd
3952	2S1254-690	Discovery of a 3.9hr period in the X-ray light curve	T. J.-L. Courvoisier A. Parmar, A. Peacock
3961	4U1323-62	Type I Burst discovered	M. van der Klis, F.A. Jansen, J. van Paradijs, W.H.G. Lewin
3980	TV Columbae	X-ray periodicity discovered in range 1-7 keV.	A.C. Brinkman, J. Schrijver
3996	2S 0142+61	1456 sec Modulation of the X-ray flux	N.E. White, P. Giommi, A.N. Parmar, F.E. Marshall

EXOSAT BIBLIOGRAPHY

Bailey, T.A., Smith, A., and Turner, M.J.L., A simple method of obtaining high background rejection in large area proportional counters. Nucl. Instrum. and Methods 115, 177 (1978).

Brinkman, A.C., Dijkstra, J.H., Geerlings, W.F.P.A.L., van Rooijen, F.A., Timmermann, C., and Korte, P.A.J., de., Efficiency and resolution measurements gratings between 7.1 and 304 Angstroms. Appl. Opt. 19, 1601 (1980).

Korte, P.A.J., de., X-ray scattering from epoxy replica surfaces. SPIE Proceedings Space Optics - Imaging X-ray Optics Workshop 184, 189 (1979).

Korte, P.A.J., de, Bleeker, J.A.M., den Boggende, A.J.F., Branduardi-Raymont, G., Brinkman, A.C., Culhane, J.L., Gronenschild, E.H.B.M., Mason, I. and McKechnie, S.P., The X-ray imaging telescopes on EXOSAT. Space.Sci.Rev. 30, 495 (1981).

Lainé, R., Giralt, R., Zobl, R., Korte, P.A.J., de and Bleeker, J.A.M., X-ray imaging telescope on EXOSAT, SPIE Proceedings Space Optics - Imaging X-ray Optics Workshop 184, 181 (1979).

Peacock, A., Andresen, R.D., Manzo, G., Taylor, B.G., Re, S., Ives, J.C., and Kellock, S., The gas scintillation proportional counter on EXOSAT. Space.Sci.Rev. 30, 525 (1981).

Sanford, P.W., Mason, I.M., Dimmock, K. and Ives, J.C., The parallel-plate imaging proportional counter and its performance with different gas mixtures. IEEE Trans.Nucl.Sci., NS-26 (1) 169 (1979)

Taylor, B.G., Andresen, R.D., Peacock, A. and Zobl, R., The EXOSAT Mision. Space.Sci.Rev. 30, 479 (1981).

Turner, M.J.L., Smith, A., and Zimmermann, H.U., The Medium Energy Instrument on EXOSAT. Space.Sci.Rev. 30, 513 (1981).

---oOo---

Turner, M.J.L. and Breedon, L.M., Spectral and temporal features in bursts from 2S1636-536 observed with EXOSAT. MNRAS (1984), 208, 29p.

Caraveo, P.A., Bignami, G.F., Giommi, P., Mereghetti, S., and Paul, J.A., EXOSAT Observation of the candidate X-ray counterpart of Geminga. Nature 310, 481-483 (1984).

White, N.E., Parmar, A.N., Sztajno, M., Zimmermann, H.U., Mason, K.O., Kahn, S.M. Evidence for 4.4 hour periodic dips in the X-ray flux from 4U1755-33. Ap.J., 238, L9-12, 1984.

Cook, M.C., Watson, M.G., McHardy, I.M. EXOSAT Observations of H2215-086: detection of the X-ray pulse period. MNRAS (1984), 210, 7p.

Ögelman, H., Beuermann, K., Krautter, J. The detection of X-rays from Nova Muscae 1983 with the EXOSAT Satellite. Ap.J., 287, L31-34, 1984.

Biermann, P., First Results from the X-ray Satellite EXOSAT. Mitteilungen der Astronomischen Gesellschaft Nr. 62, p.101-121, 1984 (Minden 1984).

Branduardi-Raymont, G., EXOSAT Observations of Active Galactic Nuclei. MPE Report 184. X-ray and UV Emission from Active Galactic Nuclei. October 1984, p. 88.

Beuermann, K., EXO1102.8+2539, an X-ray Variable AGN. MPE Report 1984. X-ray and UV Emission from Active Galactic Nuclei. October 1984, p. 111.

REPORT ON THE 'ESLAB SYMPOSIUM'

The 18th ESLAB Symposium held at Scheveningen from 5-9th November 1984 was a well-attended meeting, and illustrated the very great impact EXOSAT is making in all areas of X-ray astronomy.

Stellar Coronae

The study of X-ray emission from stellar coronae using the capability of EXOSAT to make long continuous observations has proved important. N. White (EXOSAT, ESOC) et al. reported a 35 hr observation of Algol in which they hoped to see the eclipse of the X-ray bright K4 star by the X-ray dark B8 star. The data showed only very marginal evidence for an eclipse, implying that the X-ray emission is from a region at least of a size comparable with the binary separation. A temperature of 2.4×10^7K was determined, very similar to that obtained by the Einstein SSS for the hard component. This suggests that there really are two distinct plasmas with different temperatures, rather than a continuous distribution of temperatures. A large flare originating in a $0.3R_*$ loop was observed. This size suggests that it should be associated with the cooler (7×10^6K) of the two components seen by the SSS.

O. Vilhu (Helsinki) and J. Heise (Utrecht) showed that the EXOSAT X-ray light curve of the compact binary VW Cep can be understood in terms of an X-ray luminous 'neck', the point where the two stars are in contact and through which there is a large matter flow. This is in contrast to the Einstein data, which implied one bright region on the side of one of the stars.

A. Pollock (Birmingham) briefly reviewed the observational situation of Wolf-Rayet (WR) stars which show a much greater range of X-ray luminosities than normal giants. The majority of the X-ray bright objects are in binary systems in which the X-rays probably originate in the dense interacting winds of the system. Two objects are WN7 objects exhibiting absorption lines. One more WR (HD193793) was added to the list, a WC7 + abs object, which is probably the counterpart of H2O18+439. Thus all X-ray bright WR stars are in binary systems or show absorption lines.

An invited review of the EXOSAT observations of hot white dwarfs was given by J. Heise (Utrecht). These objects are among the very brightest seen by the low energy telescopes on EXOSAT, and the count rate and 3000 Lexan: Al/P count rate ratio are extremely sensitive to temperature and helium abundance. Three objects have been observed with the gratings on EXOSAT. HZ43 shows no evidence for a 228 Å He jump and the limit on the abundance is $He/H \lesssim 10^{-5}$,

in contradiction to a previous result by Malina. The grating spectrum requires T_{eff} = 60000K, N_H = 2 x 10^{18} cm^{-2} and log g = 8. The Fiege 24 grating spectrum cannot be described by simple models. Inclusion of NLTE effects suggest that log g = 5, ie. that this is not a white dwarf, but a subdwarf. The existence of metal absorption lines in IUE spectra would tend to confirm this. The Sirius B spectrum is not simple and the measurement explains previous discrepancies between different observations. The data at 100 Å imply T_{eff} = 27000, log g = 8.3 and pure H, but there is an excess flux in the range 60-100Å.

Of the 20 objects observed using the filters to provide spectral information about half have significant counts. For some of these the count rate with the Al/P filter is larger than that with the 3000 Lexan filter, implying He/H $\gtrsim 10^{-3}$. This is difficult to understand given the rapid gravitational settling that is expected to occur. Convection or radiation pressure is presumably responsible for the observed He abundancies in these objects.

Cataclysmic Variables

K. Mason (MSSL) reviewed the dramatic increase since the launch of EXOSAT in our knowledge of the X-ray emission from magnetic cataclysmic variables (C.V.). Among the AM Her objects, EF Eri (2A0311-227) shows a hard X-ray maximum at the time of the eclipse by the accretion column and H1405-451 is similar in this respect. Many other AM Her objects appear to be relatively faint in hard X-rays. It is the soft X-ray light curves which are the most striking, in particular an observation of almost four orbital periods of AN UMa has provided a high resolution light curve showing two eclipses. The systems 1E2003+225 and H1405+451 have similar soft X-ray light curves. AM Her itself was evidently active at its other or possibly both poles when first observed by EXOSAT, although it has subsequently returned to its previously known state. The intermediate polars (DQ Her objects) were also discussed. These are systems in which the magnetic white dwarf is not rotating synchronously and a disk is present due to smaller magnetospheres than in the AM Her objects. The old nova (and now a dwarf nova) GK Per is a recent addition to this class. VW Hyi is an unusual object within the magnetic C.V.'s. It was observed to pulse coherently with a period of 14 sec and to have a temperature of the order of 10 eV during a superoutburst. This very fast period and low temperature clearly distinguish it from the intermediate polars, which have periods at least an order of magnitude longer and are primarily observed as hard X-ray sources.

The intermediate polar TV Vol (2A0526-328) has been known to exhibit 3 periods (2 photometric, 1 spectroscopic), related in the standard way for these systems to the white dwarf rotation

period, the orbital period and the beat period between the two. Schrijver (Utrecht) et al. report on an EXOSAT observation in which another period (1943 sec), in hard X-rays, was discovered. This must represent the white dwarf rotation period and so throws open the question of the origin of the other periods. Motch (Besancon) has confirmed the existence of this new period in UBV photometry.

V1223 Sgr, another intermediate polar, was shown on two occasions by Osborne (EXOSAT, ESOC) et al. to exhibit a narrow dip in X-ray intensity coincident with the peak of the rotationally modulated X-ray intensity. A similar feature has been observed in the object H2252-036. V1223 Sgr, one of the brighter of these objects, has a complex X-ray spectrum, probably consisting of 3 components in the soft and hard X-ray ranges, rather like that of GK PER. Comparison of X-ray and optical pulse arrival times leads to the conclusion that the reprocessed optical pulses probably originate in the accretion disk bright spot.

The brightest hard X-ray dwarf nova SS Cyg has been extensively observed by EXOSAT. M. Watson (Leicester) et al. presented a preliminary report in which the luminosity of the source in quiescence was said to be proportional to the square of the derived temperature. This was compared to an expected $L_X \propto T^{3/2}$ relationship based on a model by King and Shaviv of the white dwarf - disk boundary layer at low mass transfer rates and low densities. Hard X-ray emission would come from a corona surrounding the white dwarf. This model received some additional support from the observed timescale of small flares and the delay between the hard and soft X-ray intensity variation of 60 sec.

The AM Her object 1E2003+227 was discussed by K. Mukai (Oxford) et al. who presented data from La Palma, I.U.E. and EXOSAT. This is the only AM Her object for which an X-ray grating spectrum is available (apart from AM Her itself). It is characterised by a blackbody temperature of 25 eV. The UV spectra are phase resolved and show NV emission only around linear polarisation phase 0.8. The radial velocity variation of 3 distinct line components was presented and a suggestion of asynchronism of the white dwarf rotation was made, based on an observed difference in the systemic velocity from that previously published.

At the end of the session N. White (EXOSAT, ESOC) et al. presented the data from an EXOSAT observation of the soft source (=BH candidate?) 2S0142+61. This object was discovered to have a 25 minute period in the hard component of its spectrum, which is a zero energy index power law. The 0.7 keV thermal component is unpulsed. Both spectra are absorbed by 10^{22} H atoms.cm^{-2}, and one candidate optical counterpart is heavily absorbed. The spectral characteristics of this source are quite unlike those of the

intermediate polars, and indeed none of the possible optical counterparts looks like a cataclysmic variable.

AGN

McHardy (Leicester) gave a review on the current status of X-ray observations of AGNs. Large amplitude X-ray variations are uncommon: but they do occur. Rapid variability seems to be rare while longer term variability is quite common. Most Seyferts and quasars show the 'Universal power law spectrum' with $\Gamma = 1.65$ but there are exceptions - eg. 3C273 is flatter.

Bradt (MPI) presented EXOSAT observations of the OVV BL Lac object H0323+023: unfortunately no variability was observed.

Warwick (Leicester) reported EXOSAT observations of the BL Lac objects MKN 421 and MKN 501. MKN 421 showed rapid ($\lesssim 1$ day) variability: for both objects the spectrum was quite steep, ie. the high energy tails were absent.

Pollock (Birmingham) presented data of 5 high luminosity BL Lac objects, four of which varied on rapid ($\lesssim 1$ day) timescales.

Pounds (Leicester) reported on some interesting EXOSAT results of NGC 4151. Variation by a factor of 3 in the 2-10 keV flux was not seen in the LE's, indicating a second soft component below 1 keV. The ME data indicated partial covering of the continuum source by the absorbing column; this was however contested by Perola (Rome) who suggested a warm absorber.

Shafer (Cambridge) reported X-ray and optical studies of the N galaxy 3C 390.3, which has undergone a huge decrease in its Bolometric luminosity since the early 1970's: optically it is now a narrow-line radio galaxy. The X-ray spectrum seems flatter than the usual AGN power-law and either a warm absorber or partial covering are indicated.

Stewart (Leicester) discussed EXOSAT observations of the quasar MR2251-179. Variations in the ME were not coordinated with those in the CMA, suggesting separate continuum components. Similar behaviour in 3C273 was reported by M. Turner (Leicester).

Supernova Remnants

The session on SNR's was divided into discussions of objects with thermal and non-thermal emission.

B. Aschenbach (MPI) gave a review of galactic SNR's in which he highlighted the EXOSAT results on the thermal objects Puppis-A, Cas-A and Tycho. Filter spectroscopy e.g. on Puppis-A indicates small scale temperature/density variations across the remnant. M. Arnaud (SACLAY) presented CMA images of selected parts of the Cygnus Loop, processed with subtraction of background data. Vela SNR data was discussed by A. Smith (SSD); this complex region was resolved into several nonthermal components, one close to the pulsar and another centred on the maximum of the radio distribution. B. Kellett (MSSL) presented data on PKS1209-52, including PSD images. The SNR 1E1149.4-620g, serendipitously discovered by the Einstein IPC, was discussed by G. Bignami (IFC, Milan) in respect of Einstein IPC and EXOSAT CMA data. Analysis of the Tycho GSPC spectrum, presented by J. Davelaar (EXOSAT, ESOC), shows an overabundance of the low-Z elements S, Ca and approximately solar abundance for Fe.

The session on non-thermal SNR's was opened with a review by B. Becker (UCLA), who showed that the imaging data from Einstein on these synchrotron nebulae, which are similar to the Crab Nebula, confirmed the central-peaked morphology as seen in radio observations. The energetics of a sample of 8 objects show a tendency for an evolutionary sequence. VLA survey data indicates new candidates for these objects. In addition to the Einstein imaging results, EXOSAT can make a significant contribution in this area through ME (and GSPC) spectral and timing observations. The ME spectral data on SNR29.7-0.3 were discussed by L. Koch (SACLAY). The featureless power-law spectrum and the X-ray luminosity point to a relatively young Crab-like object. Spectral observations of G21.5-0.9, 3C58 and Vela, presented by J. Davelaar (EXOSAT, ESOC), show power-law spectra with a range of spectral index between 0.7 and 1.1. In combination with radio spectral data, an evolutionary sequence and the hypothesis of a single or multi-component particle input spectrum was discussed. The SNR session was concluded with a review by K. Long (ST. Sci., Baltimore) on supernova remnants in external galaxies with emphasis on the Einstein LMC survey.

X-Ray Binaries

The ability of EXOSAT to make long continuous X-ray observations is proving to be very important in the search for an understanding of the nature of the regular 'dipping' X-ray sources. M. Watson (Leicester) presented the results of an EXOSAT observation of 4U1624-69. The X-ray light curve is dominated by a series of sharp dips where the observed flux falls to ~25% of its 'normal' value. Strong changes in low energy absorption are seen during the dips but, in contrast to other sources, no dip periodicity has been detected.

T. Courvoisier (MPI Garching) showed how the dips observed from 2S1254-690 recur with a period of 3.9 hours (the same period is seen in the optical light curve); the associated spectral changes cannot be simply described by a change in low energy absorption by cold material with normal cosmic abundances and/or by a change in temperature. A. Parmar (ESOC) presented the results of a continuous 18 hour EXOSAT observation of 4U1755-33. This source shows 4.4 hour periodic spectrally independent dips with a maximum reduction in flux of 40%. This spectral independence implies an underabundance of metallic elements of about a factor 600 less than cosmic values for a point source. A model where the central X-ray source is extended was thought unlikely since the L_X/L_{opt} ratio of 4U1755-33 is 1000.

K. Mason (MSSL) presented results on the X-ray binary 2S0921-630. This source is similar to Cyg X-2 except that L_X/L_{opt} is about 1 rather than 200. An EXOSAT observation during an optical eclipse detected an X-ray flux similar to that of previous uneclipsed values, suggesting an extended X-ray source. Since the central point source must be hidden from our view, this provides a natural explanation for the low L_X/L_{opt}.

Some of the tremendously exciting EXOSAT results on Her X-1 were presented by H. Ogelman, P. Kahabka and W. Voges (MPI). Their data show evidence for a change in the average 35 day cycle duration - an important result since the mechanism responsible for this modulation is still not fully understood. The high time resolution and large collecting area of the ME has allowed the Her X-1 pre-eclipse dips to be studied in great detail. EXOSAT results show a newly discovered phenomenon of large intensity and spectral variability on a timescale of about 100 sec during the dips.

New results on the X-ray burst source 2S1636-536 were presented by M. Turner (Leicester), J. van Paradijs

(Amsterdam) and W. Pietsch (MPI). One burst was observed jointly by EXOSAT, Tenma and ESO. The importance of the continuous coverage of EXOSAT, enabling the interval between bursts to be unambiguously obtained, was emphasised.

Galactic Plane Scan

A new X-ray image of the galactic plane has been produced using the 45 arcmin square field of view of the medium energy instrument on EXOSAT. A lens-shaped region 10 degrees wide at the galactic centre and extending in longitude for 90 degrees either side of the centre was mapped using a series of 90 degree slews. This map shows a total of 64 sources including 18 new ones and the first observation of persistent emission from the globular cluster bursters Terzan 1 and Terzan 5. The most important discovery from this image is a 2 degree wide ridge of diffuse emission symmetrical about the plane and extending from the galactic centre to galactic longitude = ±40 degrees. The spectrum of this emission appears to be hard (alpha approx. 1.2) with no significant absorption.

P. Barr
J. Davelaar
P. Giommi
J. Osborne
A. Parmar
M. Turner (Leicester)

EXOSAT DATA ANALYSIS WORKSHOP

Summary of Presentations/Actions

The workshop was held at ESTEC on 12/13 November 1984, immediately following the ESLAB Symposium, and was attended by about 40 scientists active in EXOSAT data analysis. Presentations were given by Observatory Team members and SSD staff on the following aspects, and discussions highlighted a number of areas requiring additional analysis and/or calibration measurements.

- Mission Overview; Timing aspects (Internal Experiment/OBC)	D. Andrews
- FOT Structure and Data Handling	J. Sternberg
- LE Calibration	L. Chiappetti
- LE Data analysis	P. Giommi
- ME Calibration and Data Analysis	A. Smith
- GSPC Calibration and Data Analysis	A. Peacock

A few points are noteworthy:

- Analysis of dead times in the ME experiment electronics/data handling logic has revealed a discrepancy of the order of 15% between the observed loss as a function of known source count rate and theoretical estimates. Although for most purposes it is sufficient to correct the count rates according to empirical formulae, analysis of rapid variability requires a knowledge of the mechanism and further work is in progress (details in a future EXPRESS).

- Spectral fitting of LE data from the Crab has demonstrated a good overlap with the ME results under the assumption of a $N_H = 3 \times 10^{21}$ cm^{-2}.

- Boron filter effective area (ref. p. 31).

- ME deficit of counts in channels 4-7 of spectra. Difference spectra show features consistent with the background lines - is this variability of the lines ? Additional work is in progress.

- CRAB LE test tape produced and despatched.

- Telescope FOV obscuration - further study in progress.

- UV contamination assessment continues.

- CMA gain depression: calibration (raster scan planned).
- Blank field/filter to be produced and written to calibration tape history.
- ME resolution functions to be checked.
- Error in GSPC Bi line energies (ref. p. 25).
- Channel 0/1 inconsistency in FOTH; next revision.
- Table of OBC work space parameters defining spectrum integration times for relevant ME modes to be provided.

As noted in the foreword our intention is to hold a second Data Analysis Workshop at ESOC provisionally from 16-18 April 1985. Readers are invited to contact the Observatory for more details and to indicate topics for inclusion in the discussions.

D. Andrews

GSPC CALIBRATION UPDATE (ref. EXPRESS no. 6, p. 18)

Background Line Energies, Subtraction and Detector Gain

Further work on Cas A has quite clearly demonstrated that the two lines in the background are caused by the $L\alpha$ and β transitions of Bismuth. These lines arise from the activation of the lead collimator material to Pb^{210} which then decays with a half life of 4 days to Bismuth to give the observed L emission lines. The energies of these lines are 10.83 and 13.01 keV respectively (averaged over the α_1, α_2, β_1, β_2 branching ratios of 100, 10, 50 and 20).

Experience now shows that, except for extremely bright sources (e.g. Sco X-1), the channel number of the 13.01 keV line can be established to within one channel (gain 2.0) by fitting two gaussian lines and a polynominal of order 3 or less to the data. The same is true for the 10.83 keV line although for some brighter sources the uncertainty in the measured channel number may increase (e.g. for a bright bulge source). The 13.01 keV line can be reliably used to lock the gain of the GSPC for any particular observation. Photomultiplier stimulation data should be used to check only the gain drift throughout an observation.

It has been found that the apparent energy of the 4.75 keV feature, when fitted as a line, depends by up to 10% on the shape of the underlying continuum. It is now unnecessary to fit this feature which should be included directly in the response matrix, by overlapping the energies of the matrix by 70 eV at 4.78 keV.

The Effective Areas

Analysis of several long exposures on the Crab in October and November this year produced further refinement of the effective areas. A series of splined three order polynomials were fitted to the Crab data in order to force the response to give the correct fit. The increased exposure time for a burst length window of channels 89-107 of 25800 s has revealed some small deficiencies in the previously quoted values. The revised values are given in Table 1 and are good to a systematic uncertainty of 1%.

An update to the CCF is in progress and will be distributed as soon as possible (details in the next EXPRESS).

N.E. White

Table I: GSPC Effective Area

Energy	89-104	89-107
1.6	.072	.223
1.9	1.040	1.591
2.2	4.644	5.363
2.5	9.722	12.757
2.8	15.611	20.190
3.1	22.336	28.424
3.4	30.464	38.072
3.7	36.348	45.553
4.0	41.842	53.136
4.3	46.024	58.534
4.6	50.498	63.463
4.9	54.328	68.758
5.2	55.477	70.439
5.7	58.087	74.514
6.2	62.543	79.298
6.7	65.880	83.188
7.2	67.803	86.548
7.7	70.007	89.545
8.2	72.351	90.589
8.7	75.331	91.819
9.2	75.859	92.550
9.7	77.415	93.926
10.2	78.601	94.427
10.7	78.435	94.526
11.2	78.255	94.225
11.7	78.016	93.531
12.2	77.676	92.455
12.7	77.194	91.014
13.2	76.471	89.154
13.7	75.592	87.040
14.2	74.466	84.686
14.7	73.192	82.249
15.2	71.346	80.093
16.2	66.658	76.419
17.2	61.906	71.541
18.2	57.218	66.080
19.2	52.723	60.579
20.2	48.484	55.412
25.2	31.338	39.613
30.2	20.485	25.894
35.2	54.906	69.404
40.2	44.888	56.741
45.2	36.476	46.107
50.2	29.604	37.421
55.2	24.082	30.440
60.2	19.779	25.002
65.2	16.311	20.618
70.2	13.614	17.209
75.2	11.431	14.449
80.2	9.633	12.176

THE EXOSAT SUM SIGNAL EFFICIENCY CORRECTION : DIRECT COMPUTATION FROM THE DATA

Readers not familiar with the CMA sum signal and its usage to compute the sum signal-dependent efficiency correction are referred to the FOT Handbook, section 8.1.3 for an introduction. The basic facts are summarised below, then a new method (not described in the FOT Handbook) to compute the efficiency correction directly from the data, without the use of the CCF, is presented.

The sum signal is the summed output from the readout contacts on the CMA resistive disc. It appears as an ADC channel number (0-127) for each event in the IM packet. Since only events with a signal above a given threshold (PET=Position Encoding Threshold) on any of the four contacts are considered valid, a sum signal histogram (counts vs ADC channel no.) will start abruptly at a given ADC channel, which is a function of the PET setting (so far constant) and of the position in the field of view.

Events in channel 0 and 1 are spurious and should be disregarded. Since the CMA efficiency given in the CCF was calculated using no PET, a correction is necessary for a sum signal-dependent factor. This is simply the ratio between the area of the sum signal distribution above the threshold, and the total area (with no threshold). This method was used to generate the correction factors in the CCF from the ground measurements (monochromatic X-rays).

Data analysis at the EXOSAT Observatory has shown that the values in the CCF are only guidelines to the in-flight behaviour (cosmic sources are not monochromatic!). In particular, for a given sum signal distribution and its median, the correction factor obtained from the CCF is underestimated in comparison to the directly computed value.This implies that a larger correction is necessary, i.e. the actual correction coefficient (which is a number between 0 and 1) is lower (further from 1) than the predicted value.

The difference is small for most of the normal X-ray distributions (for which the correction factor is in any case close to 1), but could be non-negligible for softer distributions (lower sum signal median).

The following method may be used to compute the efficiency correction directly from the data. It assumes that a Pearson type 1 distribution describes the source sum signal

distribution; this is confirmed in practice. Naturally, the parameters of the Pearson distribution are different from those for a monochromatic distribution. No attempt has been made to model the sum signal distribution from a continuum as a convolution of monochromatic distributions: the Pearson fit provides a good empirical description.

1) Accumulate a signal histogram $y=f(x)$ using a set of values y_i for each channel $i=0,127$. The associated sum signal value may be derived as $x_i=i-0.5$.
2) Locate the threshold to define the first channel to be fitted. This can be done very easily by eye, or an automatic algorithm may be developed.
3) Fit the data with the modified Pearson type I distribution

$$y = K \left(1 + \frac{x - x_0}{a_1} \right)^{m_1} \left(1 - \frac{x - x_0}{a_2} \right)^{m_2}$$

where the five parameters K, x_0, a_1, m_1, m_2 are variable and the following relation holds $m_1/a_1 = m_2/a_2$. A least squares fit method (e.g. Bevington's CURFIT) can be used.

4) The following assumptions are valid as initial parameter values:

K = height of the peak of the distribution
x_0= channel of the peak of the distribution
a_1= x_0
m_1= ratio between the first channel (from the top) with at least 10% of the peak counts, and x_0
m_2= m_1

The above guesses generally lead to a quick convergence. In a few specific cases the values require some adjustment (generally try to raise m_1 and m_2, i.e. make the distribution narrower). To select the initial parameters by eye, please note:

K controls the peak height,
x_0 and a_1 control the peak position,
m_1 and m_2 control the skewness of the left and right wing of the distribution.

5) Once the above parameters are calculated, the threshold for integration should be determined.

One possible method is to calculate the channel numbers

corresponding to 80% and 20% of the histogram value at the threshold used for the fit (point 2 above). The values may be determined in fractional channel numbers using the y values for two adjacent channels (one above and one below 80% or 20%), the x values defined according to the convention at point 1 above, with a linear extrapolation. Further linear extrapolation can be used to derive a fractional channel number (corresponding to 50% of the initial y value at the threshold), which is the integration threshold.

6) Integrals of the fit on all the channels and on that part above the threshold determined at point 5 are computed. A straightforward numeric integration (histogram summation) is sufficient.

7) The efficiency correction is the ratio of the two integrations.

The above is used by the program EFCOR in the EXOSAT Observatory LE Interactive Analysis System.

L. CHIAPPETTI

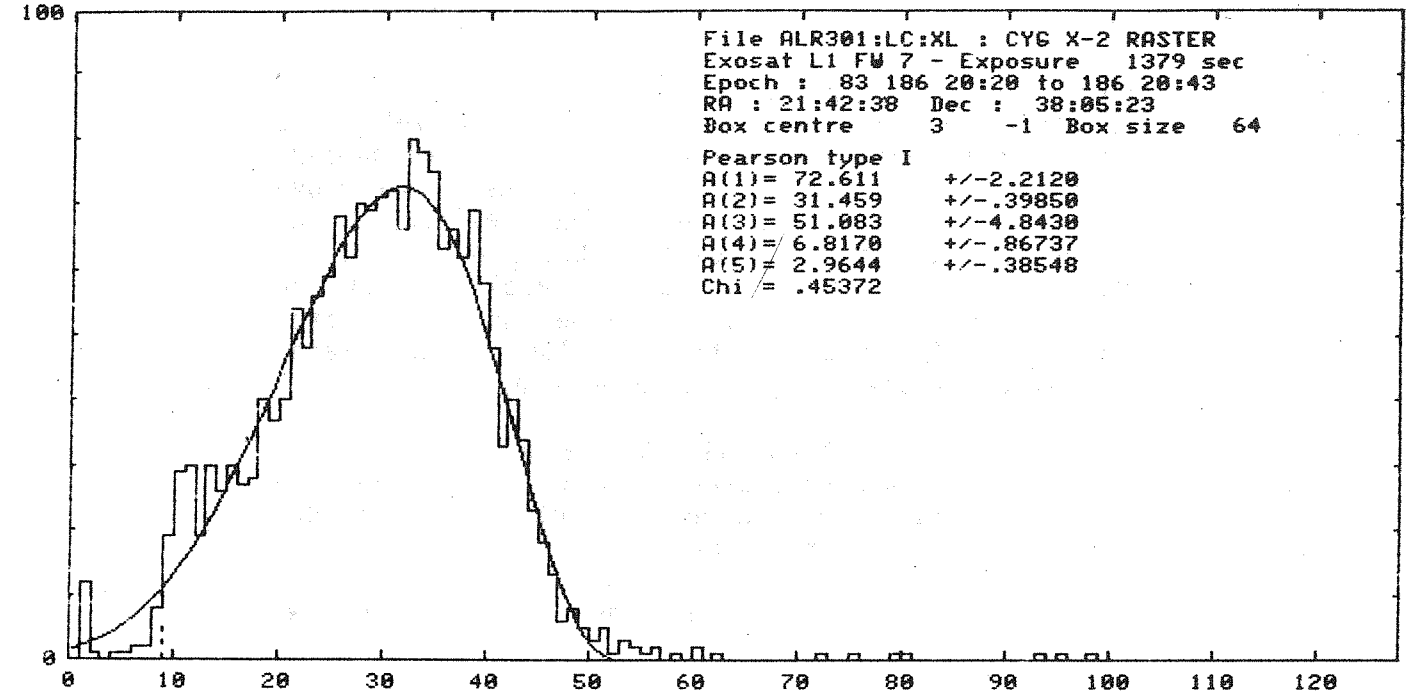

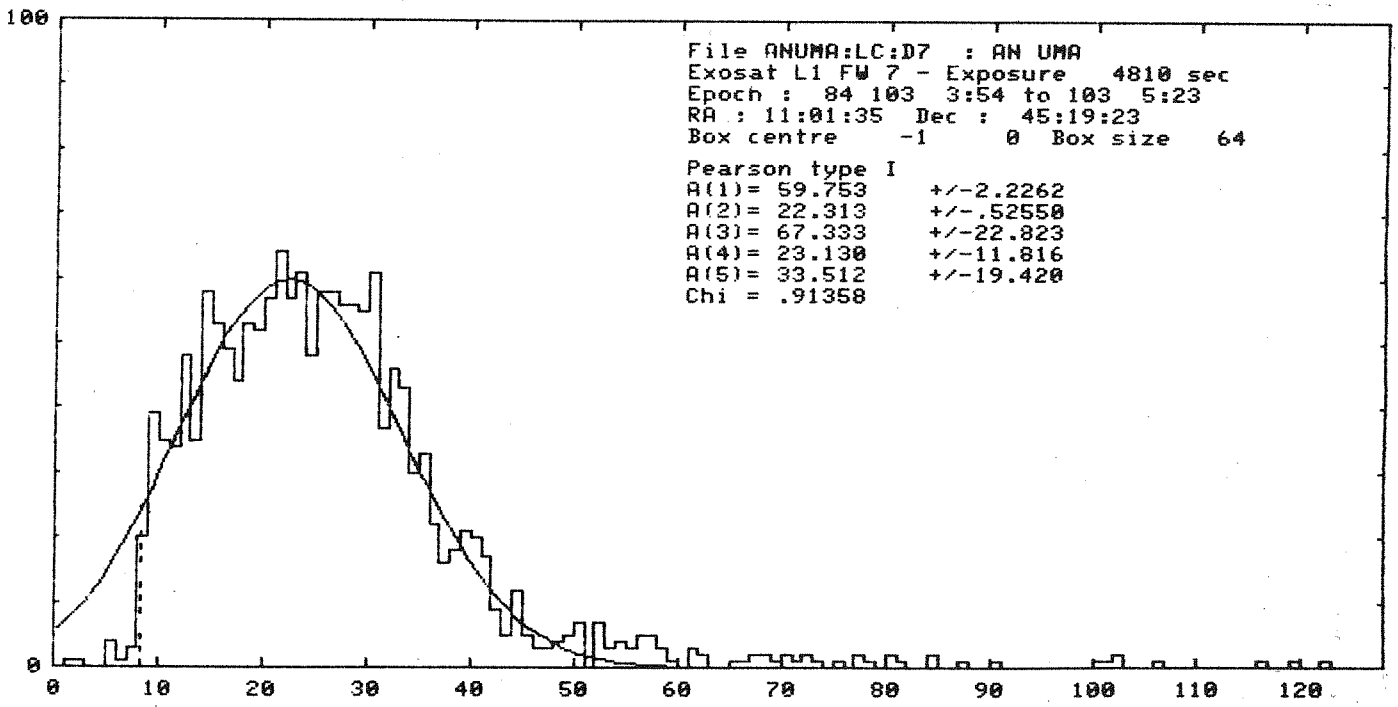

The top frame shows a sum signal histogram (and its Pearson fit) for a hard X-ray source (Cyg X-2). The integration threshold is at channel 9.0, and the efficiency correction 97.4 % (compared with a CCF value of 98.8 % obtained from the sum signal median value of 30.5).
The bottom frame refers to a softer source (AN UMa). The integration threshold is at channel 8.4 and the efficiency correction is 92.7 % (to be compared with a prediction of 97.4 % using the sum signal median of 25.0).

THE BORON FILTER EFFECTIVE AREA

Participants at the ESLAB Symposium may have noticed that a few speakers referred to a "problem" with the effective area of the CMA used in conjunction with the Boron filter. A brief account is given here of the status of the problem, similar to a presentation at the Data Analysis Workshop held in ESTEC in November, and a few points are added to indicate current work.

a) The Ground Calibration

For all filters, the calibration analysis had been conducted at the Space Research Laboratory, Utrecht. For each filter the mass absorption coefficient, the absolute thickness and the thickness as a function of position were determined. A number of measurements at different (monochromatic) energies were used as a starting point.

Analysis of the Boron filter data is quoted as "the most accurate available", however the higher intrinsic complexity of the boron filter should be noted.

Most of the filters are a single layer of a pure material. The Al/Par filter is two separate layers plus a support grid and can be described in a relatively simple manner (ref. FOT Handbook, section 8.1.1.3). On the other hand, the Boron filter is made of Boron in an organic solvent, sprayed on a polypropylene support, and description by separate components was therefore not possible. Modelling was necessary to describe it as a single effective component. The model was based on a number of measurements, one at an energy just below the Boron edge and six at higher energies.

b) In-Flight Verification

Note the Boron effective area features (e.g. see Fig Ec, in the FOT Handbook, section 8.1): there is a significant window below the Boron edge, then the oxygen and carbon edges are clearly visible with the bulk of the transmission around 1 keV.

A comparison of calibration measurements of the Crab Nebula with predicted count rates leads to a good agreement (see FOT Handbook, section 8.1.1.5). However, since the column to the Crab is quite high (3×10^{21} cm^{-2}), this simply verifies the higher energy part of the effective area.

Some more calibration measurements were made on a soft X-ray source, the hot white dwarf HZ43. It is possible to obtain a spectral solution consistent with the grating measurement carried out during the performance verification phase. The spectrum derived from the grating observation and the CCF area gives a predicted Boron count rate of around a factor 10 higher than the measured one.

The same problem (predicted count rate higher than observed) has occurred in some observations of soft sources like catalysmic variables, or AGN's with very low column density.

A sample of AGN's has been analysed with 1.7 power law spectrum and column density derived from two additional LE filters, usually 3000 Lexan and Al/P. The discrepancy between the predicted and observed count rates in the Boron filter is dependent on N_H, ranging from a factor $\sim$2.5 at 5×10^{19} cm^{-2} to 1.3 at 3×10^{20} cm^{-2}.

Checks of the filter ratios on HZ43 with the known grating spectrum and for a few other soft sources have been carried out.

One current area of investigation is the Boron filter point spread function which is found to be broader than the CCF values, possibly resulting from scattering within the filter. Checks are in progress to assess the influence on count rate estimates.

L. Chiappetti
J. Davelaar

A GUIDE TO THE INTERACTIVE ANALYSIS SYSTEM

1. General

In the period 01/12 to 31/12, several groups of visitors to the Observatory made use of the interactive analysis system and their experience, together with that of the Observatory Team, has led to a few general guidelines for the organisation and proper exploitation of the system.

Users are reminded that the IA system was implemented primarily as a facility whereby the community could analyse EXOSAT data in more detail at the Observatory. There is no question of the Observatory Team undertaking a systematic interactive analysis (in the absence of the user) of data as a service - this is the function of the automatic analysis. It is recommended that users of the system should as far as possible be familiar with general X-ray data analysis techniques, since the support provided by the Observatory Team is geared in general towards a demonstration of the facilities rather than a 'supervision' of the entire analysis. First time users are expected to require a few hours full time advice from the Duty Scientists followed by consultancy support on specific details.

Real time interactive analysis of LE data will not be supported because of the excessive time required to linearise the image.

During the the system trial period, which will terminate on 15.03.85, no real time booking will be permitted, i.e. P.I.'s attending their current observation must request IA system time in advance in the normal manner (EXPRESS no. 7, p. 43). Only one 'observer' will be allowed access to the system at any one time although one observer means in practice one or two 'bodies'. From 15.03.85 to 31.03.85 the Observatory Team require 100% access to the computer system for configuration, co-ordination of final updates and testing and documentation such that a full service will be provided from 01.04.85.

Throughout the night period (23.00-08.00) no support of the IA system is in principle available, although the Observatory Controller will be able to offer some advice, consistent with the real time DCR operations having priority at all times.

Note that the software comprising the IA system is not an Observatory product, but rather a means of production and as such is not available for distribution outside the Observatory.

2. The ME Interactive Analysis System

A description is given of the facilities that are supported, or will shortly be supported by the ME Interactive Analysis System. The two basic end products of the ME interactive analysis are spectral and rates files. These are used by a series of analysis programs, common to all the instruments, for spectral fitting, period searching, plotting etc.

Data from the following OBC modes can be analysed with the system: HER2, HER3, HER4, HER5, HER6, HTR3, PULS, PLS2, DIR2. Note that for the pulsar programs only spectral analysis can be carried out at present and for DIR2 only a very simple analysis is possible.

a) Spectra

The data used to create a spectral file can be selected in the following ways:

1 - Argon or Xenon data
2 - Particular Detectors
3 - Time, phase or count level windows

Background subtraction can be carried out using:

1 - Slew data
2 - Array swap data, corrected for offset
3 - Standard CCF spectra
4 - Leicester University background correlations

The detector gains are stored on the spectral file at the time of creation so that the effects of detector gain drifts and pre-amplifier gain setting changes are 'hidden' from the user. In addition, deadtime correction factors can be measured or calculated and applied to the spectra. Once a spectral file has been produced it can be plotted or used as an input to the spectral fitting program.

b) Light Curves

Light curve or 'rates' files can be produced with the following options:

1 - Argon or Xenon
2 - Integration interval
3 - Energy channels (or bins)
4 - Method of background subtraction (as for spectra)

In addition, the difference in intrinsic background counting rates can be corrected for using either array swap or slew data or standard background files. The file can be deadtime corrected and for some OBC modes the deadtime correction factors can be a function of time. The times stored in a rates file can be corrected to heliocentric times; note that Madrid is assumed to be at the centre of the world and the Sun at the solar system barycentre.

The rates files can be used as inputs to the following programs:

1 - Fourier Analysis
2 - Folding Analysis
3 - 'Publication Quality' Plotting
4 - Interactive Timing analysis facility

c) Other Facilities

Other important facilities supported by the ME Interactive Analysis include:

1) Directory listings - Listings of times, OBC modes pointings of all the observations on a FOT etc.

2) Observation Information - More detailed listing for a selected observation

3) HK Analysis - Plots and listings of any spacecraft or experiment HK parameters

4) Macros - Commands can be executed from a file. Parameters can be set at execution time allowing the use of standard macros

5) Help files - On-line documentation of each command

d) Future Improvements

The ME Interactive Analysis was designed to be used by a small number of scientists each of whom would be very familiar with all aspects of the operation of the ME, the OBC, the HP computers and the OP analysis environment. As

many of the astronomers coming to use the interactive analysis will not be familiar with these, much work is currently underway to improve the help files and level of documentation. In addition, analysis of high time resolution data is very time consuming mainly because of the low CPU power of the HP computers. A link to the ESOC Fujitsu main-frame computer has been established and it is expected that many of the CPU intensive processes will be transferred from the HP's to the Fujitsu

3. The LE Interactive Analysis System

The LE Interactive Analysis System consists of more than 10 programs to enable users to perform all the basic operations needed for the detailed analysis of CMA data.

The following is a list of the main options offered by the system:

- Accumulate images
- Deblur images
- Accumulate sum signal histograms
- Calculate efficiency correction (see p. 27 for further details)
- Accumulate rate files*
- Rotate images
- Overlay images
- Automatic source detection
- Source centroid
- Signal to noise ratio optimisation
- Source intensity estimation and significance of detection
- Hot spot removal
- Gaussian smoothing
- Image contouring
- Pixel ↔ celestial coordinates conversion
- Count rate ↔ flux conversion

Several interactive programs suitable for the control of colour display devices are also available.

Documetation describing the LE interactive system is currently being written and will be available at the Observatory in the near future. A two-level help file and some documentation macros are already available on the HP4 computer system at ESOC.

* Accurate timing analysis of CMA data can be performed using LE rate files as inputs to the ME or GS timing programs or to the timing interactive system that is currently in preparation.

4. The GSPC Interactive Analysis System

Facilities available:

1 - Accumulate spectra for HEBL2 data
HEBL4
DIRECT (old)

2 - Accumulate rate buffers for HEBL2, HEBL4, HK data.

3 - Background subtract spectral buffers and determination of detector gain.

5. General Facilites

1) Spectral Fitting - One or two detectors up to a maximum of 256 channels. Detectors that are currently supported are GSPC, ME and all CMA filters (the latter are counted as one detector).

2) FFT - a 4096 point fast Fourier transform can be applied to the rates buffers generated by the various IA programs. For data sets longer than 4096 points the FFT's are summed together.

3) Folding - An unlimited amount of data can be folded over 75 trial periods and a plot of χ^2 as a function of period obtained together with a plot of the light curve of the period with the best χ^2.

4) Light curves - a general purpose folding (at a single period) and light curve program will data for three detectors at once.

5) Timing analysis interactive system (currently in preparation and testing) common to all instruments with the following objectives:

a - 'chain' the data (bad data, fill in gaps with simulated data etc. and eliminate long term trends).
b - test the hypothesis of constancy by various statistical tests (χ^2, % variability) and determination of the source statistical moments.
c - search for flares/bursts (down to msec).
d - search for periodicities and determination of folded light curves.
e - phase fitting for pulsating sources.
f - characterise aperiodic variability via autocorrelation function techniques.

g - investigate amount of variability as a function of energy and spectral changes.
h - correlate data from different energy bands or experiments via cross correlation function techniques.

D. ANDREWS
P. GIOMMI.
A.N. PARMAR
L. STELLA
N.E. WHITE

EXOSAT AND THE FITS TAPE FORMAT

The FITS format is described in two papers in volume 44 of Astron. Astrophys. Suppl. It specifies a way of encoding simple data structures on magnetic tape, but intentionally avoids addressing the question of what happens to that data within any computer system. "Simple structure" means FORTRAN array(s) with header(s). Some aspects of the FITS format are open to criticism, but its merit is that its clear documentation minimises the possibility of misunderstanding the contents of the tape.

The EXOSAT Final Observation Tape, on the other hand, contains data structures that are not simple according to this definition and are generated by on-board hardware or software (not FORTRAN). In contrast to the FITS approach, the observer is advised to preserve these structures on disc and in the memory of his computer, since the FOT Handbook and all distributed software refer to these structures.

A number of users of EXOSAT data have commented on the difficulty of "reading" (by which is meant "understanding and correctly using") EXOSAT Final Observation Tapes, and ways of giving more assistance in this area have been and are still being investigated. No application has yet, however, been found for the FITS format. Some of the reasons are:

- the importance of time variability (requiring preservation and distribution of data in raw form rather than accumulated results).
- the need to preserve all options for rebinning or selecting data (note e.g. that a full image would be a 2048x2048 array, which would generally occupy more space and contain less information than the original events on the FOT).
- the need for telemetry to be archived and distributed in a way which does not depend on calibration data (the definition and knowledge of which is still undergoing improvement).

The situation is rather different for analysis results. For example, using the EXOSAT interactive system, it is possible to save the intermediate or final results (images, spectra etc.) to disc in a format which would be convertible to FITS tapes. The implementation of a means for observers to take away such results on tape is under consideration. However, it is important to realise that

(i) the layout of such files may evolve;

(ii) the production of such files is a part of the interactive system and cannot be done retrospectively for the whole telemetry stream;
(iii) it is often in the derivation of these results where most of the effort and decisions lie - not in their subsequent use;
(iv) the types of processing which are common in X-ray astronomy are not always the same as in other areas of astronomy, hence the use of software systems developed for other projects may not be appropriate.

To summarise: the complexity of EXOSAT FOT's reflects the complexity of the EXOSAT payload and flexibility of the on-board software. It is important that users appreciate the rationale of the FOT and recognise that FITS is not a magic solution to simplifying EXOSAT data analysis.

J.R. Sternberg

OBSERVATORY TEAM

		Ext.
David Andrews	Observatory Manager	705*
Julian Sternberg	Observatory Software	703
Julian Lewis	System Software/HP Computers	702
Nick White	Senior Observatory Scientist	764
Paul Barr	Duty Scientist/Mission Planning	711
Jaap Davelaar	"	710
Paolo Giommi	"	715
Manfred Gottwald	"	758
Julian Osborne	"	714
Arvind Parmar	"	763
Luigi Stella	"	716
Anne Fahey	Mission Planning	707
Paolo Ferri	Observatory Controller	772
Maria Gonano	" "	772
Frank Haberl	" "	715
Geoff Mellor	" "	772
Antonella Nota	" "	716
Mark Sweeney	" "	772
Susanne Ernst	Data Assistant	713
Margit Farkas	" "	709
Grazia Giommi	" "	709
Linda Osborne	" "	713
Sandra Andrews	Secretary	704

*Direct dialling to any extension, prefixed by 886, is possible, eg. 06151-886-705

Personnel Changes (01.11.84-31.12.84)

Dr. L. Chiappetti's leave of absence from his home institute has terminated and he has returned to IFC, Milan.

OBSERVATORY TEAM RESPONSIBILITES/POINTS OF CONTACT

D. Andrews	Day-to-day management, organisation and running of the Observatory
J.R. Sternberg	Observatory software; FOT production and organisation; FOT Handbook; Observatory log
J.C. Lewis	Observatory computer system software; Hardware, networks, links etc.
N.E. White	Science Research Observatory Team science focus and co-ordination of scientific output GSPC instrument calibration and performance overview GSPC IA analysis software development and maintenance
Duty Scientists	General : Science Research Operation support Interactive Analysis System Support Orbit Preparation/Liaison with P.I.'s
P. Barr	Mission Planning TOO's; real time changes; 'special' observations; s/w maintenance
J. Davelaar	LE1 calibration; UV contamination; area, filter response; spectral analysis
P. Giommi	LE instrument calibration and performance overview; LE IA software design/maintenance; CMA background analysis
M. Gottwald	ME collimator response; ME/GS auto s/w maintenance; general facilities: library, optical plates, EXOSAT output (PR)

J. Osborne	LE cal., PSF/sum signal; real time graphics s/w; LE auto and cal s/w maintenance; grating software maintenance.
A. Parmar	ME instrument calibration/performance overview and OBC operational aspects; ME interactive analysis software development and maintenance; ME calibration: area/efficiency/ resolution
L. Stella	Timing analysis; off-line (Fujitsu) processing; clock stability

Observatory Controllers

P. Ferri M. Gonano F. Haberl G. Mellor A. Nota M. Sweeney	Real time DCR operations; instrument health monitoring; assistance with specific calibration aspects; software development
A. Fahey	Mission Planning: Generation of time lines; coordinated observation planning; liaison with P.I.'s

Data Assistants

Susanne Ernst Margit Farkas Linda Osborne Grazia Giommi	FOT administration and despatch; auto-analysis organisation and running; auto output despatch; IA system booking, tape handling; maintenance of Observatory catalogues/ address lists etc.; computer system maintenance, consumables, disc space etc.
S. Andrews	Observatory secretary

QUESTIONNAIRE

☐ There is an error in my name or address on the current mailing list; the correct version is given below.

☐ Please add my name and address (printed below) to the EXOSAT Express mailing list.

☐ Please delete my name and address (printed below) from the EXOSAT Express mailing list.

NAME: _____

ADDRESS: _____

_____

_____

_____

Tear off the page and return to: EXOSAT Observatory, ESOC, Darmstadt.